JOURNAL OF MATERIALS SCIENCE 23 (1988) 4319–4330.

Effect of testing conditions and microstructure on the sliding wear of graphite fibre/PEEK matrix composites

PARIMAL B. MODY, TSU-WEI CHOU
Materials Science Program and Center for Composite Materials, University of Delaware, Newark, Delaware 19716, USA

KLAUS FRIEDRICH
Polymers and Composites Group, Technical University Hamburg-Harburg, West Germany

The sliding friction and wear behaviour of unreinforced polyetheretherketone (PEEK) matrix and its unidirectional continuous and two-dimensional woven graphite fibre-reinforced composites were investigated. The operating wear mechanisms, as evinced by scanning electron microscopy of the worn surfaces, and the coefficients of friction and the wear rates changed considerably with the fibre reinforcement form and orientation. Sliding wear rates, on account of their extreme sensitivity to the microstructure of the interacting surfaces at the sliding interface, were found to be a function of not only the surface roughness, but also of the sliding time. Complex interactions arising due to the effects of the testing parameters such as fibre orientation, sliding velocity, contact pressure and interface temperature were characterized for the neat matrix and the two composite systems. The wear rates of the two-dimensional woven composites were almost an order of magnitude lower than those of the unidirectional fibre composite or the unreinforced matrix.

1. Introduction

The main reward of advanced thermoplastic composites in tribological applications lies in their often self-lubricating properties, high specific strength and stiffness, chemical inertness, ability to dampen shock and vibration, and above all, amenability to tailor the material for specific applications. In recent years, the focus has shifted from a mere substitution of conventional metals by polymers to the development of specific polymer matrices and fibre reinforcements, along with the engineering of their various combinations.

In sliding wear, material loss is primarily dominated by adhesive mechanisms, and secondarily, by surface fatigue and abrasion; the abrasive component increases with increasing surface roughness. As compared with the abrasive wear conditions, wear processes here are much milder – lower by almost five orders of magnitude [1] – and are, consequently, extremely sensitive to the microstructure of the surface being worn. Each material possesses its own characteristic microstructure that is likely to cause a unique tribological behaviour. This is especially true for composite systems.

When two surfaces interact, contact is made at the asperities on the two surfaces. With the application of a normal load and relative motion, surface contaminants and films are removed, plastic deformation at the asperity contact zones occurs, causing new surfaces to be created. As a result, adhesive junctions are formed which, under the influence of motion, tend to get fractured. Fracture occurs not at the original point of contact, but at some point within the softer material. Hence material is transferred from one surface to the other. Subsequently, these transferred particles come loose due to the repeated contact, and may be back-transferred as well. Sliders, bearings, gears and cams are some of the common applications where this type of sliding or adhesive wear is encountered.

While relatively fewer efforts have been aimed at investigating the abrasive wear of polymers and their composites [2–4], their sliding wear behaviour has been receiving the bulk of attention on account of their wider gamut of practical applications. Sliding velocity (v) effects are manifested in frictional heating that is generated at the sliding interface. At some critical velocity, steady-state wear will no longer prevail, and the coefficient of friction and/or the wear rate will increase sharply. Reinforcing fibres usually increase the critical velocity of polymers [5]. The influences of contact pressure (p) on sliding wear and of temperature on limiting pv values have been investigated by Anderson [6] and Wolverton *et al.* [7], respectively. Humid environments can cause wear rates to either increase or decrease, depending on the polymer system [8]. Counterface properties as characterized by the surface roughness, number of asperity peaks per unit area, slope and height of the asperites, etc., and the state of the sliding interface as characterized by the presence or absence of lubricants and

0022–2461/88 $03.00 + .12 © *1988 Chapman and Hall Ltd.*

transfer films and their properties, are also of paramount importance in determining the operating friction and wear mechanisms.

The issue of fibre reinforcement raises three important parameters: fibre form, volume fraction and fibre orientation with respect to the sliding direction. Carbon fibres usually lower wear rates of composites for two reasons: the fibres (a) support a bulk of the applied load and (b) smooth the steel counterface by a mildly abrasive action. However, in most systems, wear-reducing effects by fibres are limited up to a critical volume fraction which value depends on the fibre–matrix combination. Above this value, wear either remains steady or may increase, as in glass fibre-reinforced systems. These observations have been recorded for short-fibre composites [9–11], and for continuous fibre composites [10]. Almost all investigations on unidirectional continuous fibre systems have concentrated on differences among in-plane longitudinal (or parallel), in-plane transverse (or anti-parallel), and normal orientations. Hybridization of unidirectional fibres has been shown to result in a positive synergism in wear properties [12]; the experimental wear rates were lower than the prediced values.

Woven forms of fibre reinforcement have been demonstrated to yield superior wear characteristics in specialized applications. Grove and Budinski [13] discussed the choice of a fabric form of fibre reinforcement for a self-lubricating bearing, and Gardos *et al.* [14] employed a three-dimensional weave of graphite fibres while designing a self-lubricating turbine bearing for application at high temperatures. While the friction and wear behaviour of polymers [15] and their short and unidirectional continuous fibre systems [16] have been researched, documentation of a systematic approach to studying the friction and wear of woven fibre composites under adhesive-dominant conditions (achieved by sliding against smooth steel surfaces) is very limited, if not non-existent, and warrants more attention. This paper presents an investigation of the principal component of the sliding friction and wear of a neat thermoplastic matrix (PEEK), and examines changes achieved by the incorporation of unidirectional continuous and two-dimensional woven graphite fibres. The differences in behaviour with different forms of fibre reinforcements and orientations are explained in terms of fundamental mechanical processes of material removal, and of the observed wear mechanisms on worn surfaces.

2. Experimental details

2.1. Materials

The unreinforced polyetheretherketone (PEEK) matrix, its unidirectional continuous, and its two-dimensional woven graphite fibre-reinforced composite systems were tested. Table I describes the materials in greater detail.

2.2. Testing procedures

A Falex friction and wear testing machine (pin-on-disc type) was employed for the sliding wear tests. Besides the testing machine, a control unit was present which monitored the specimen temperature, the torque generated at the sliding interface, the sliding velocity (in terms of revolutions per minute), the sliding distance (in terms of the number of revolutions made), and the sliding time. Frictional torque, monitored through the entire length of the test, was plotted on a plotter interfaced with the control unit. Fig. 1 shows a close-up of the specimen configuration. The specimen was attached to a specimen-holder, and this integrated unit was fixed on to the testing machine as seen. The sliding counterface was a polished steel surface. The surface topography was generated by random polishing over a wet 600-grit silicon carbide abrasive paper corresponding to an average centre-line-average roughness of 0.06 μm at the beginning of each test.

In a series of initial experiments conducted to determine the effect of sliding time on wear, for three different surface roughnesses, results showed that initially, wear progressed in a non-linear fashion. Later, as a definite sliding interface was established, steady-state conditions prevailed, and the mass loss (Δm) increased linearly with increases in sliding time. In order to lend credibility to quantitative comparisons of wear rates and coefficients of friction of the different material systems employed, measurements were made within this steady-state regime. This was definitely reached after a sliding duration of 75 min. In addition to this test period, an initial run-in sliding duration (of 15 to 30 min) was performed on each specimen to ascertain that all of its apparent area was in contact with the counterface. Subsequently, four runs were made for each of three identical specimens corresponding to a specific combination of testing parameters.

All material systems were subjected to identical combinations of testing parameters which are summarized in Table II. For a given contact pressure,

TABLE I Description of the material systems employed

Type	Material	Fibre modulus (GPa)	V_f (%)	ϱ (g cm^{-3})
Matrix	Polyetheretherketone (PEEK)*	–	–	1.32
Unidirectional fibre composite	AS4 graphite fibre/PEEK*†	235	60	1.57
2D woven fibre composite	HTA7 graphite fibre/PEEK† (five-harness satin weave)	235	60	1.57

*Supplied by ICI, UK.
† Received as prepregs and pressed into laminates.

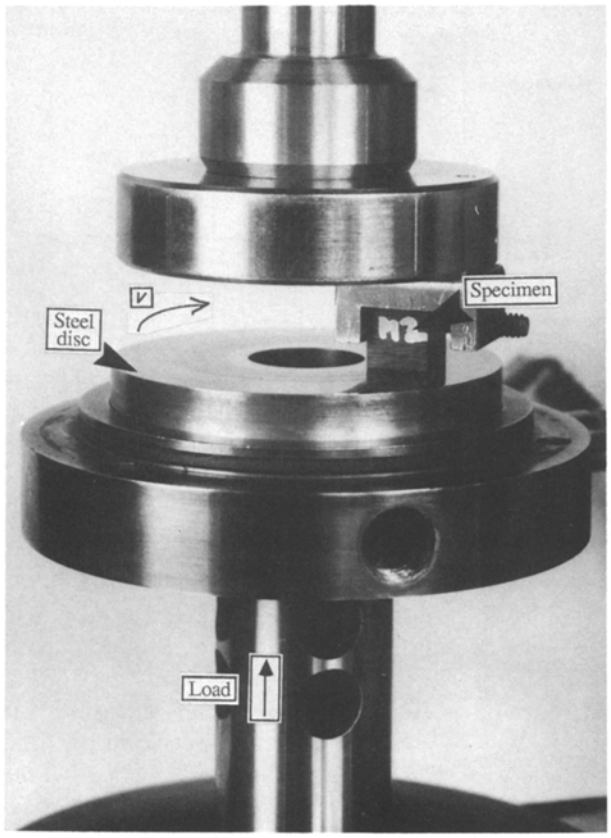

Figure 1 A close-up view of the specimen configuration in sliding wear.

various sliding velocities were tried until the highest one that did result in a stabilized coefficient of friction (and interface temperature) was achieved. This value of sliding velocity established an upper bound over an arbitrary range selected. Various levels of contact pressure were then tried out to maximize the operating contact pressure for this range of sliding velocities, without disturbing the stability of the coefficient of friction (or the interface temperature). This process hence ensured operation under possibly the most severe but steady-state conditions. The temperature at the sliding interface was monitored by a thermocouple placed at a point within the steel disc and approximately 1.7 mm below the sliding surface. In all room temperature tests, forced air cooling was employed to maintain the interface temperature at 50° C. However, external heating was used to generate the higher interface temperatures.

TABLE II Test parameters for the sliding wear experiments

Parameter	Type/range
Test apparatus	Pin-on-disc
Specimen size	8.9 mm × 8.9 mm × 8.9 mm
Sliding counterpart	1018 steel, HRC 20, R_a = 0.06 μm
Orientations	as in Fig. 2
Sliding velocity (v)	0.5/1.0/1.5 m sec^{-1}
Contact pressure (p)	0.6 MPa
pv factors	$pv1$ = 0.3 MPa m sec^{-1}
	$pv2$ = 0.6 MPa m sec^{-1}
	$pv3$ = 0.9 MPa m sec^{-1}
Interface temperature	50/150/240° C
Sliding duration	75 min
Humidity	30% r.h.

2.3. Sliding directions

The sliding directions are outlined in Fig. 2. Three principal directions for the unidirectional continuous fibre composite were identified, and are shown in Fig. 2a. Fibres in the plane of sliding and parallel to the direction of sliding were termed parallel (P). In-plane fibres oriented transverse to the direction of sliding were termed anti-parallel (AP), and fibres that stood normal to the plane of sliding were designated as normal (N).

For the woven fibre system (with a five-harness satin weave), six sliding directions were defined, as depicted in Fig. 2b. The longitudinal or warp direction of the fabric which had 80% of the in-plane fibres oriented in the direction of sliding, and 20% transverse (P/AP surface), was referred to as the parallel direction (P). On the other hand, the weft or width direction of the fabric that had 80% of the in-plane fibres transverse and 20% parallel (AP/P surface) was referred to as the anti-parallel direction (AP). Having thus defined the P and AP directions for the woven fibre system, consider a face perpendicular to the warp direction. This face will have a combination of fibres that stand normal to it, and parallel or transverse depending on the direction of sliding on this face. Similarly, for the face orthogonal to the weft orientation of the fabric, the same reasoning prevails. From Fig. 2b it can also be concluded that the pair $N_{P(N,P)}$ and $N_{P(N,AP)}$ is the same as the pair $N_{AP(N,P)}$ and $N_{AP(N,AP)}$, if the warp and weft fibre yarns are the same fibre type, which was the case here. (The entities within the parentheses represent fibres of those orientations which are being slid).

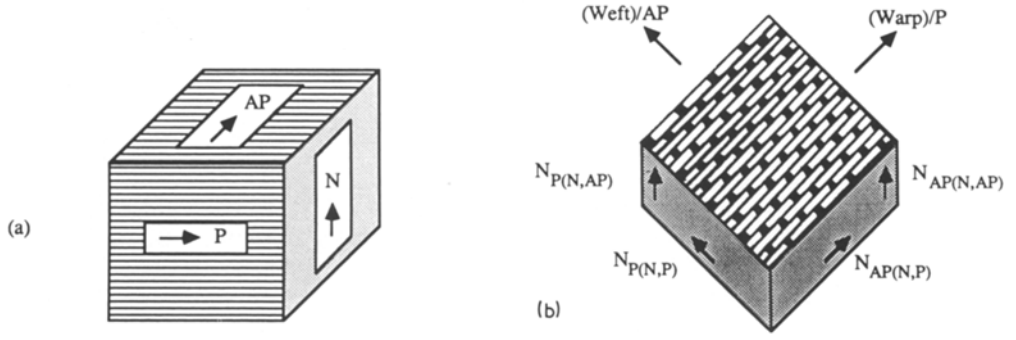

Figure 2 Sliding directions with respect to the fibre orientation for (a) the unidirectional continuous fibre composite, and (b) the two-dimensional woven fibre composite.

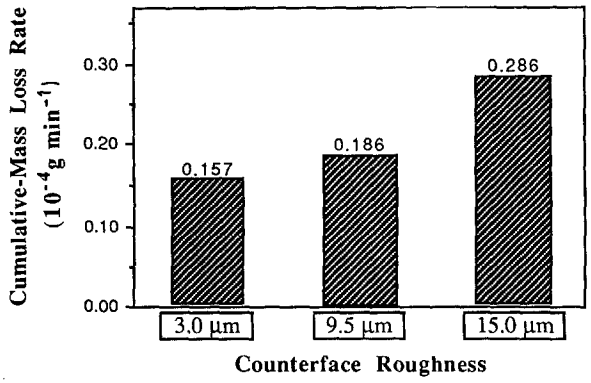

Figure 3 Effect of counterface roughness on wear. P/AP woven surface, pv = 0.6 MPa m sec^{-1}.

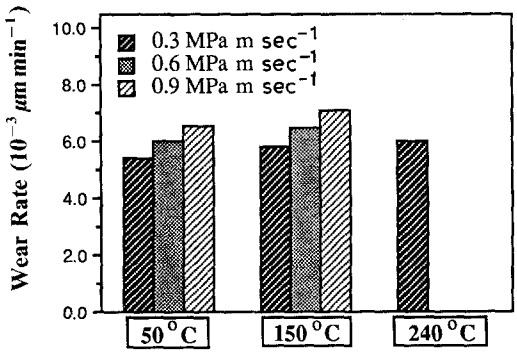

Figure 5 Variation of the wear rate of unreinforced PEEK with temperature and pv.

2.4. Wear equation

The dimensionless wear rate (w), given the units of μm m^{-1} (depth worn per unit distance slid), was computed by using the measured entities, mass loss (Δm) and density (ϱ), along with the apparent contact area (A) and the sliding distance (L) in the following form

$$w = \Delta m/(AL\varrho) \quad (1)$$

The wear resistance of a material, often referred to, is the reciprocal of the wear rate (w^{-1}).

2.5. Scanning electron microscopy

The worn surfaces were examined to determine the operating friction and wear mechanisms, and were gold-coated prior to observation. Arrows on the micrographs presented in this paper indicate the direction of sliding on the specimen surface.

3. Results

3.1. Coefficient of friction and wear rates

3.1.1. Counterface roughness and sliding time

The counterface roughnesses were varied for two reasons: firstly, to investigate their influence on friction and wear, and secondly, to determine, from their relative differences, one counterface roughness to be used for subsequent experiments. Three different surface roughnesses were produced; the surface marked "15.0 μm" was randomly polished on wet 600-grit abrasive paper, and the surfaces marked "9.5 μm" and "3.0 μm" were polished on polishing wheels using alumina particles of the same size. Therefore, the last-mentioned surface was the smoothest and the first-mentioned, the roughest. The average wear over the three counterfaces for a P-oriented woven specimen after a sliding time of 140 min was determined; these results are shown in Fig. 3. Differences in wear for the two smoother surfaces was not significant, and highest wear was caused, quite expectedly, by the roughest surface. However, in terms of the actual mass loss measured, only the "15.0 μm" surface yielded quantities large enough to minimize errors in weighing. Consequently, this surface was chosen as the counterface roughness for all subsequent experiments. Although variations in the coefficient of friction were small ($\Delta\mu$ = 0.033), a trend was seemingly visible: it increased with increasing roughness.

The variation of mass loss of the specimen with sliding time is shown in Fig. 4 which also indicates the running-in period and the steady-state regime of wear. While the initial wear increased quickly and non-linearly, the rate of increase of wear decreased continuously with time, declining to a steady-state linear range after having slid for about 60 min. Based on this result of onset of steady-state wear, a sliding duration of 75 min was chosen for all the subsequent tests.

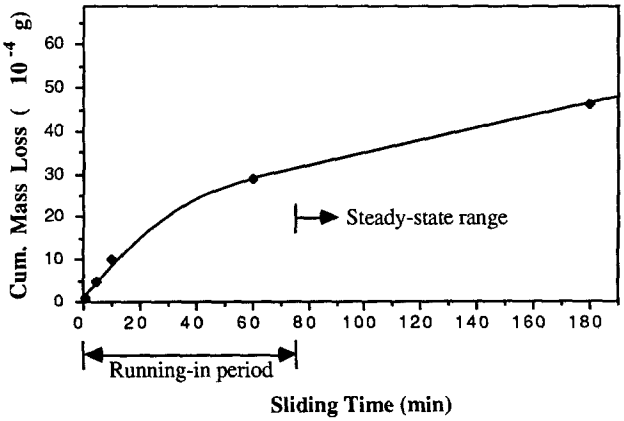

Figure 4 Effect of sliding time on the cumulative mass loss of the specimen. Orientation P, pv = 0.6 MPa m sec^{-1}, 2D woven graphite/PEEK. (◆) 15.0 μm.

3.1.2. Interface temperature and pv values

3.1.2.1. Unreinforced PEEK matrix. The variation of the wear rate and of the coefficient of friction as a function of the pv values and temperature are presented in Figs 5 and 6, respectively. The increases in the pv values corresponded to increasing sliding velocities at

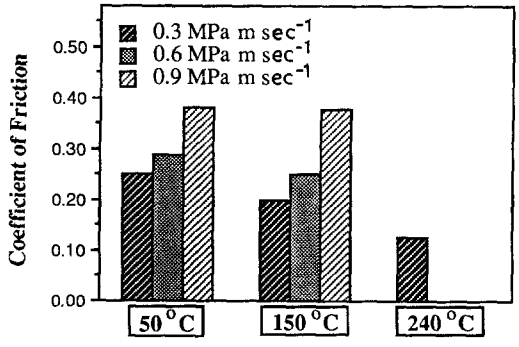

Figure 6 Variation of the coefficient of friction of unreinforced PEEK with temperature and pv.

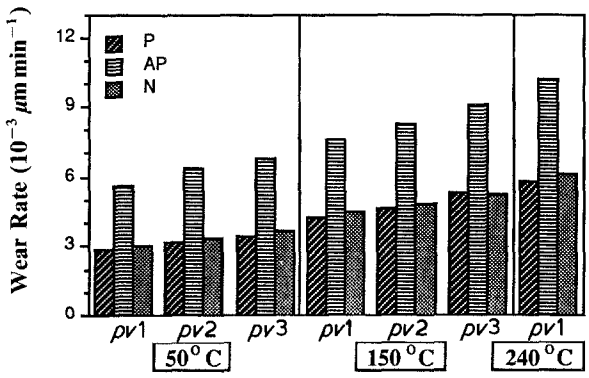

Figure 7 Variation of the wear rate of the unidirectional composite with temperature and *pv*.

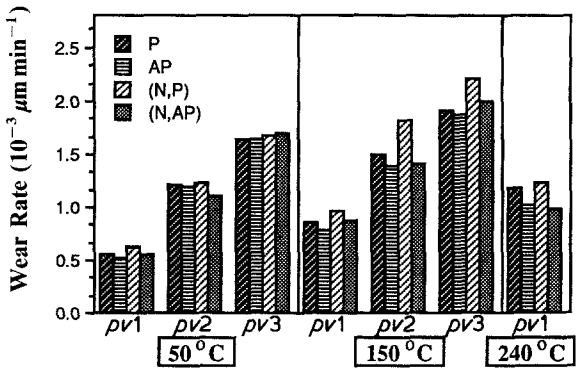

Figure 9 Variation of the wear rate of the 2D woven composite with temperature and *pv*.

a constant contact pressure. The wear rates increased with increasing *pv* and with increasing temperatures. However, the coefficient of friction increased with increasing *pv*, but decreased with increasing temperature.

3.1.2.2. Unidirectional continuous fibre composite. The wear rates and the coefficients of friction of the unidirectional fibre composite as a function of fibre orientation, *pv* product and temperature are shown in Figs 7 and 8. For all three orientations, wear increased with increasing *pv* and temperature. The P-orientation showed the least wear rates, the N-orientation was slightly higher, while the AP-orientation was much higher than both. At all temperatures, the gradation of properties between orientations was retained. Fibre reinforcement was definitely helpful in augmenting the wear resistance of the polymer, the only exception being the AP-orientation which displayed a wear rate larger than that of the unreinforced polymer. The coefficients of friction (Fig. 8), on the other hand, evinced little dependence on *pv* or temperature; however, all orientations for the composite displayed coefficients higher than for the unreinforced polymer.

For both the composites tested, the materials reached their limit of operation at 240° C with the first *pv* value tested. Sliding conditions at higher *pv* values did not allow the coefficient of friction to stabilize, prompting the conclusion that the "limiting *pv*" had been attained. Consequently, only one combination of the *pv* product was employed at this temperature for all the material systems.

3.1.2.3. Two-dimensional woven fibre composite. Owing to the equivalence of the sliding directions $N_{P(N,P)}$ to $N_{AP(N,P)}$, and of $N_{P(N,AP)}$ to $N_{AP(N,AP)}$, four unique sliding directions for the woven composite were identified. Basically, they comprised the P-oriented surface, the AP-oriented surface, a surface containing a combination of N and P-oriented fibres (N, P), and the fourth which contained a combination of N and AP-oriented fibres (N, AP). Results showing the variation of the wear rate and of the coefficient of friction for the woven composite as a function of temperature and *pv* values are given in Figs 9 and 10.

At 50° C, a high degree of isotropy was displayed in wear properties which persisted over the range of *pv* tested. At this temperature, it was really difficult to isolate the most wear resistant orientation. The coefficients of friction exhibited much higher variations among the orientations, and generally increased with increasing *pv* values. At higher temperatures, the closeness in values of the wear rates for the different orientations still prevailed at the lower *pv* values. At higher *pv*, and at higher temperatures, the woven surfaces possessing N-oriented fibres slightly stood out as the higher wearing ones.

3.2. Wear mechanisms

3.2.1. Unreinforced PEEK

Increases in *pv* as a result of higher sliding velocities could have caused enhanced microcutting of the polymer by the steel asperities resulting in increased wear. With higher interface temperature, wear rates also increased, primarily due to a degradation of the mech-

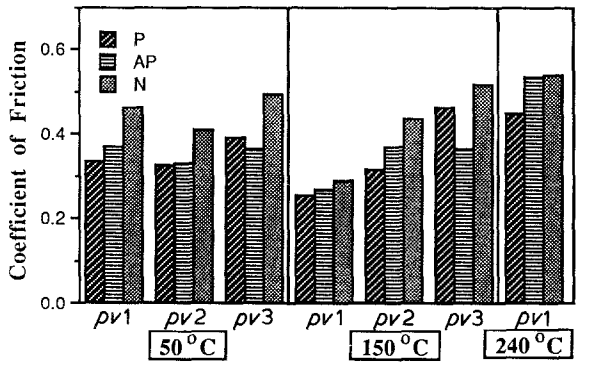

Figure 8 Variation of the coefficient of friction of the unidirectional composite with temperature and *pv*.

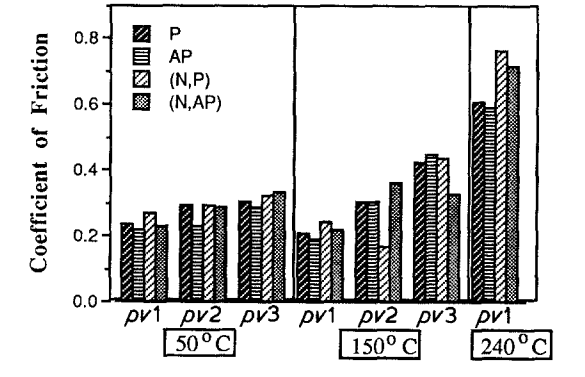

Figure 10 Variation of the coefficient of friction of the 2D woven composite with temperature and *pv*.

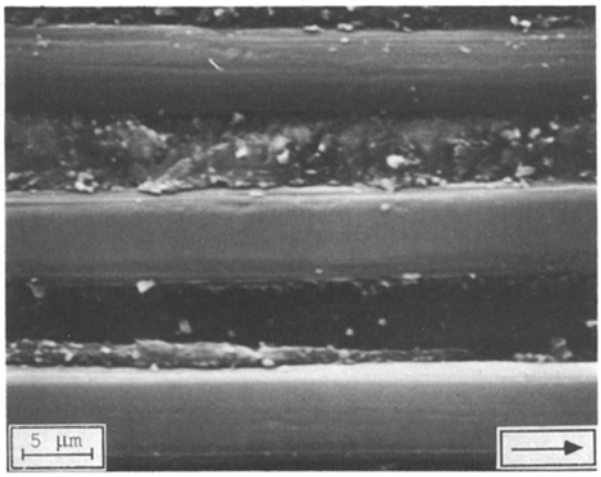

Figure 11 P-oriented fibres on a worn unidirectional composite surface.

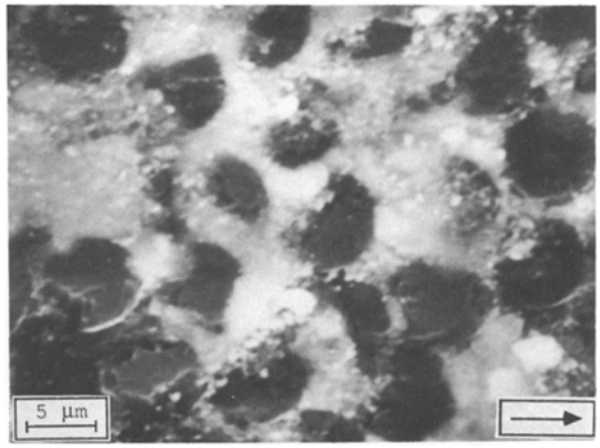

Figure 13 N-oriented fibres on a worn unidirectional composite surface.

anical properties of the polymer, which obviously could not be equalized or overcome by a simultaneous decrease in the coefficient of friction with temperature (contrary to the observations made by Voss and Friedrich [17]). The reduction in coefficient of friction is the result of frictional melting of the polymer surface regions, causing a hydrodynamic film to be built up at the interface, with lubricating effects on the sliding process. However, only a continual loss of material from the specimen could give rise to greater amounts of transferred films; hence the discrepancy in the trends of friction and wear with temperature.

3.2.2. Unidirectional continuous fibre composite

At 50° C, the P-oriented composite did not suffer much damage, and the fibres adhered well to the matrix throughout the test. However, the surrounding matrix areas were worn first leaving the fibres standing out to support a major proportion of the load (Fig. 11). On the other hand, the AP-oriented composite underwent severe forms of damage mechanisms like fibre cracking, fibre fracture, and fibre–matrix cracking leading to fibre removal (Fig. 12). Although significant amounts of back-transferred polymer was seen on the worn surface, it did not have a mitigating effect on the fibre damaging processes. In the case of the N-oriented composite, the matrix wore away first leaving short stubs of fibres in contact with the sliding interface. Subsequently, wear debris, comprising mainly of the worn polymer, became trapped between the short protruding stubs of the fibres and could have provided a cushioning effect (Fig. 13). This orientation showed higher wear rates than the parallel case because at some point in time during the sliding, the short stubs of fibre broke away and caused the whole process to be repeated again. Similar observations have been made for metal matrix composites [18].

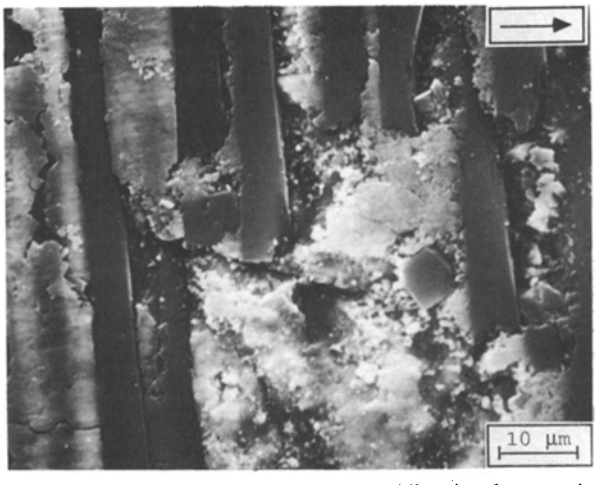

Figure 12 AP-oriented fibres on a worn unidirectional composite surface.

At higher temperatures, the gradation of properties between orientations was retained, and, for a given *pv* level, the absolute values of wear rate were higher than at 50° C. This can be attributed, on the one hand, to the enhanced wearing of the matrix material around the fibres, which, in turn, would result in faster action of the fibre-related wear mechanisms. Secondly, it can be assumed that with increasing temperature, some degradation of the fibre matrix interface occurs, which enables an easier removal of slid fibre parts after breakage into individual pieces. The same explanation holds for the trends observed with an increase in *pv* at a given temperature range.

3.2.3. Two-dimensional woven fibre composite

A comparison of the wear rates of the unidirectional and two-dimensional composites yields a clear benefit of fibre reinforcement for the second group at each temperature level and *pv* product. This should also be detectable on the worn surfaces in a way that the mechanisms observed for the unidirectional composite orientations do not simply add up when going to the two-dimensional case. The simultaneous occurrence of different orientations on the woven surface seems to lead to a synergistic behaviour, that is, wear protective performance of the differently oriented fibre regions to each other. In fact, this has been observed while analysing a variety of different wear surfaces for the two-dimensional woven composite.

3.2.3.1. P/AP woven surface. This surface was comprised of 80% in-plane fibres oriented parallel to the

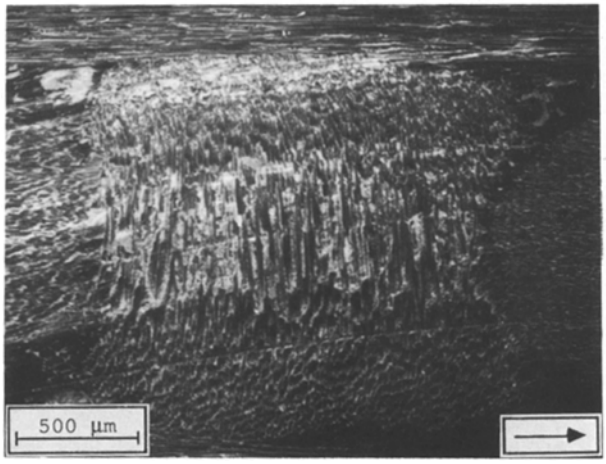

Figure 14 Wear of the cross-over region when slid over a "3.0 μm" counterface.

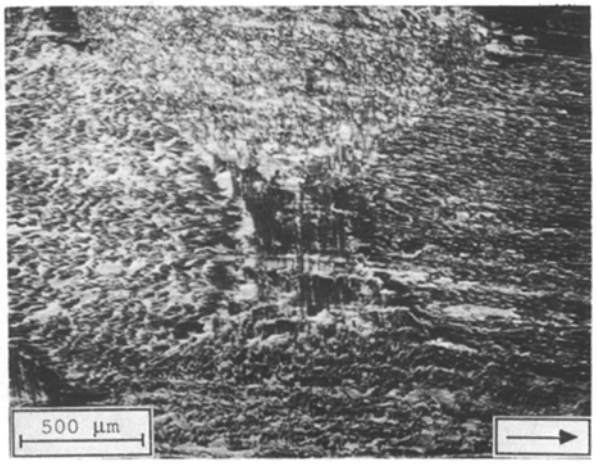

Figure 16 Wear of the cross-over region when slid over a "15.0 μm" counterface.

direction of sliding, and 20% in-plane fibres oriented transverse to the direction of sliding. Highest wear occurred at the cross-over points, with not such a dramatic action occurring far away from it. This phenomenon was, in fact, observed on specimens that were slid over three counterface roughnesses (Figs 14 to 16); there was a distinct change in size of the cross-over regions. As the roughness of the surface increased, so did the wear in the cross-over regions, and caused the higher wear rates. Quite notably, the amount of wear debris (back-transferred film) trapped within the AP-oriented fibres in the cross-over region also increased with the roughness of the counterface.

Within a given specimen, the P-oriented fibres suffered varying degrees of damage depending on their location with respect to the cross-over point. Relatively little damage was inflicted upon these fibres that were away from the region of cross-over (Fig. 17). However, as the P-oriented fibre bundles approach a region of cross-over, a small amount of an N-component is introduced into their directionality, that is, they are not 100% in-plane; consequently, wear increased at these points (Fig. 18). Although fibre fracture and fibre cracking occurred, broken pieces of fibre were still adhered to the composite surface, bringing about a lesser mass loss. Another characteristic feature of the worn P-surface was the differing amounts of transfer film deposited at various sites. The AP-sections of the P-surface acted as recipients for almost all the wear debris which consisted primarily of agglomerated polymer wear particles. These transfer films served to protect the AP-oriented fibres from extensive damage. Yet, instances of fibre cracking were not altogether uncommon.

3.2.3.2. AP/P woven surface. This surface was comprised of in-plane fibres 80% of which were oriented transverse and 20% of which were oriented parallel to the direction of sliding. Once again, large amounts of transferred polymer wear debris were observed in the AP-regions of the worn surface. However, for this surface, the wear debris was cohered in smaller lumps, as opposed to larger lumps in the case of the P/AP woven composite. No wear debris was trapped by the P-oriented fibres, which did not suffer much damage either.

3.2.3.3. N/P woven surface. Also referred to as the (N, P)-orientation, this woven surface contained 50% in-plane fibres oriented parallel to the direction of sliding, and 50% fibres standing normal to the plane of sliding. This surface was also characterized by differing amounts of transfer films deposited on the surface (Fig. 19); greater amounts were deposited on

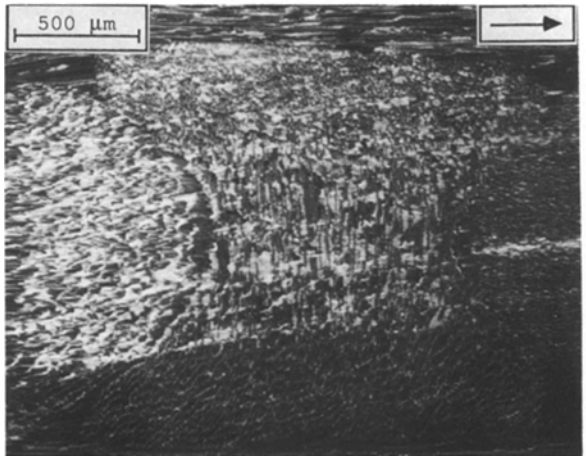

Figure 15 Wear of the cross-over region when slid over a "9.5 μm" counterface.

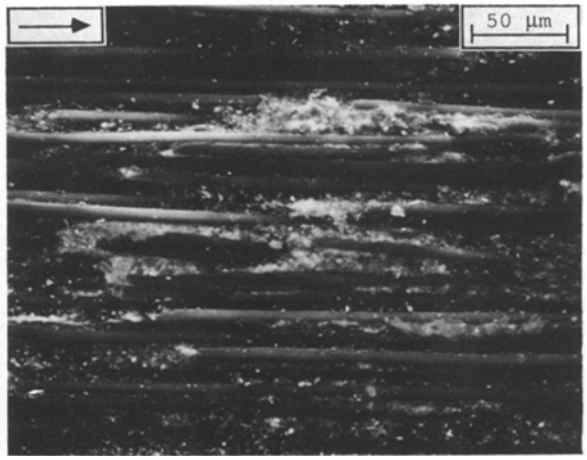

Figure 17 P-oriented fibres away from a cross-over point on a worn P/AP woven composite surface.

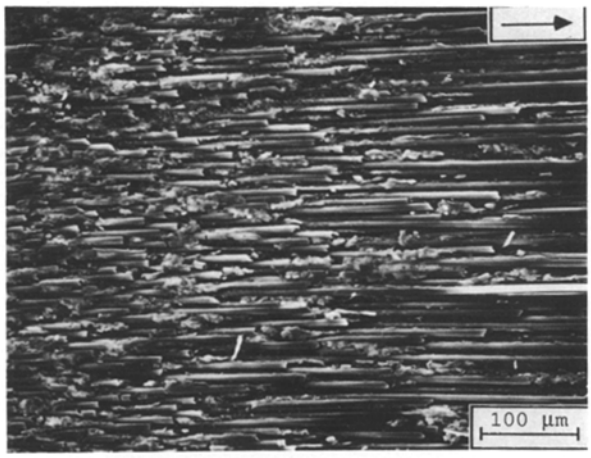

Figure 18 P-oriented fibres near a cross-over point on a worn P/AP woven composite surface.

the fibre orientation that required more of it – the N-orientation. However, not much wear debris was trapped by the P-oriented fibres which did not suffer much damage either. The wear-shielding action by wear debris in the N-oriented section of the woven composite surface was identical to that seen in the N-oriented unidirectional composite. The matrix material was worn from the P-section of the surface and deposited among the protruding N-fibres.

3.2.3.4. N/AP surface. This surface possessed a combination of 50% fibres standing normal to the plane of sliding and 50% in-plane fibres oriented transverse to the direction of sliding. Wear on this surface, also referred to as the (N, AP)-orientation, was characterized by large-scale deposition of transferred material. Both constituent orientations possess a tendency for trapping wear debris. This is a typical case of synergism that was observed in the woven composites in a sense that the wear-reducing mechanisms (shielding by wear debris) added up to yield a lower wear rate than would result from a simple mixture of the two constituent orientations.

Therefore, while identical wear rates, at 50° C, for the four sliding directions were evinced, different mechanisms were responsible for the mitigation of wear in each case. At higher temperatures, lesser

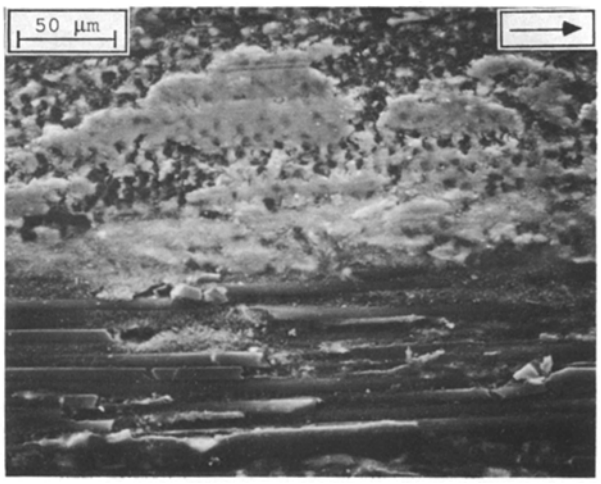

Figure 19 Worn surface of a N/P woven composite surface.

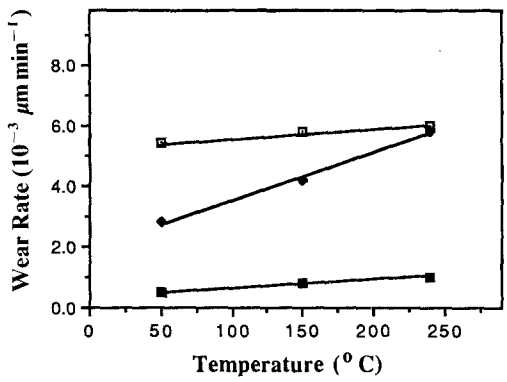

Figure 20 Variation of the wear rate with temperature. pv = 0.3 MPa m sec^{-1}. (□) Neat PEEK, (◆) UD (P), (■) woven (AP).

transfer was in evidence for the P/AP and the AP/P woven composite surfaces. However, greater amounts of transferred material were seen on the steel counterface. For the (N, AP)-oriented composite, greater amounts of transfer occurred on the N-fibres than on the AP-fibres. Consequently, damage to fibres was greater in the AP-region than in the N-region. On woven surfaces slid at 240° C (pv = 0.3 MPa m sec^{-1}) little evidence of transfer films was found. Frictional melting at the sliding interface facilitated an increased matrix flow on to the counterface. As a result, the AP-fibre bundles were not bound as tightly as would be the case at lower temperatures. Consequently, their cracking and fracture occurred with relative ease and higher wear rates prevailed for this case. The coefficients of friction were also extremely high, possibly due to increased instances of adhesion (on account of greater melting of the polymer) at the sliding interface.

4. Discussions

4.1. General remarks on the friction and wear data

4.1.1. Wear rate trends

The variation of the wear rate with temperature (at pv = 0.3 MPa m sec^{-1}) of the most wear-resistant orientations of the two composites as compared with that of PEEK are given in Fig. 20. Likewise, the variation in wear with pv product (at T = 50° C) is shown in Fig. 21. In both cases, the wear rates increased with increasing temperature and pv values. In fact, this was the trend for all orientations. Clearly, the woven composite was more wear resistant than the

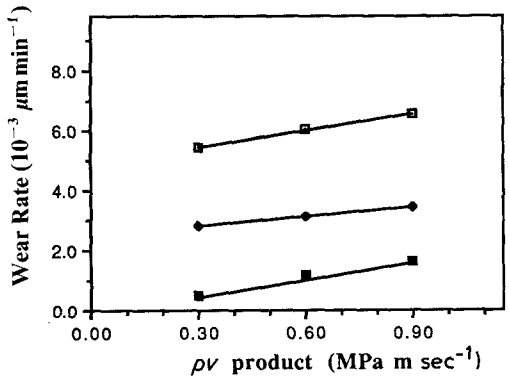

Figure 21 Variation of the wear rate with pv, at T = 50° C. (□) Neat PEEK, (◆) UD (P), (■) woven (AP).

unidirectional composite or unreinforced PEEK. Also, the woven composite was shown to be less sensitive to increases in temperature than the other systems (by comparing the slopes in Fig. 20). This suggests that the woven fibres impart a higher integrity to the microstructure of the composite at elevated temperatures. However, all materials behaved identically with increases in *pv* values.

Wear resistance increased with the incorporation of fibres into the neat matrix. The enhancement increased from two-fold in the case of the unidirectional composites, to over five-fold in the case of woven composites. The average variation among the different material systems was as follows

$$w_{\text{UD-PK}} \approx 0.52\, w_{\text{PK}}$$

$$w_{\text{2D-PK}} \approx 0.18\, w_{\text{PK}}$$

The P and N-oriented unidirectional composites showed almost identical wear rates, and very little differences prevailed among the four orientations of the woven composites. The relative wear rates of the different orientations for the two composite systems were as follows

unidirectional (UD) graphite/PEEK composite:

$$w_{\text{P}} \approx w_{\text{N}} \approx 0.5\, w_{\text{AP}}$$

two-dimensional (2D) woven graphite/PEEK

composite: $w_{\text{P}} \approx w_{\text{AP}} \approx w_{(\text{N,P})} \approx w_{(\text{N,AP})}$.

4.1.2. Coefficient of friction trends

The coefficients of friction of unreinforced PEEK decreased with increasing temperature. In the cases of the composites, the coefficients of friction registered a minimum at 150° C, and increased sharply thereafter (Fig. 22). With *pv*, the friction increased with increasing values, but not very significantly (Fig. 23). Of note, however, was the observation that the coefficient of friction of the woven composite was less sensitive to increases in *pv* than the other two material systems. In most of the cases, the coefficients of friction had values between 0.2 and 0.4, with some exceptions: the N-oriented unidirectional composite (at 50° C) and the N-oriented unidirectional and the AP-oriented woven composites (at higher temperatures).

Generally speaking, there were no clear distinctions between the coefficients of friction of PEEK and those

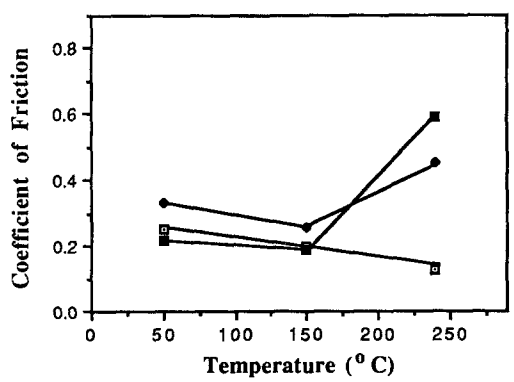

Figure 22 Variation of the coefficient of friction with temperature. *pv* = 0.3 MPa m sec^{-1}; (□) neat PEEK, (◆) UD (P), (■) woven (AP).

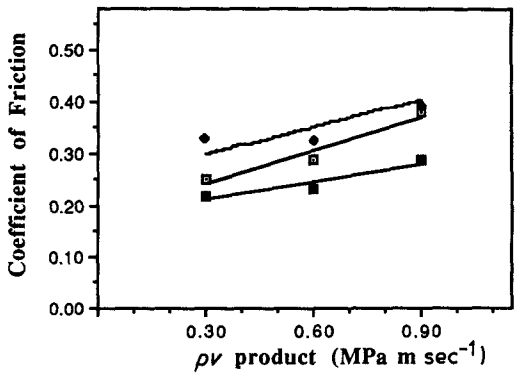

Figure 23 Variation of the coefficient of friction with *pv*, at T = 50° C. (□) Neat PEEK, (◆) UD (P), (■) woven (P).

of the two composites. There were no significant differences between the various sliding directions either, as the following indicate

unidirectional graphite/PEEK composite:

$$\mu_{\text{P}} \approx \mu_{\text{AP}} \approx 0.8\, \mu_{\text{N}}$$

two-dimensional woven graphite/PEEK composite:

$$\mu_{\text{P}} \approx \mu_{\text{AP}} \approx \mu_{(\text{N,P})} \approx \mu_{(\text{N,AP})}$$

4.2. Model for wear: unidirectional compared to woven composites

Sliding wear mechanisms are extremely sensitive to the microstructural features on the surface. Consequently, significant differences in the coefficient of friction and the wear rate occur between not only different materials, but also between various sliding directions.

Fig. 24 highlights the different mechanisms involved in wear with different fibre orientations. For all orientations, the majority of the matrix material was worn away initially leaving the fibres on the sliding interface to support the bulk of the normal load. In the P-oriented case, the fibres were in the direction of sliding; the cracks and fracture paths were perpendicular to the direction of sliding. Therefore, while there were instances of fibre fracture, fibre removal was minimal because it was not facilitated. In the AP-oriented case, the transverse fibres suffered an impact type of damage by the steel asperities. Subsequently, debonding at the interface, due to repeated sliding contact, assisted removal of the fractured pieces of fibre. P-oriented fibres, by virtue of their placement, are not subjected to this type of loading, and hence show little evidence of damage. In the N-oriented case, shielding of the specimen surface by wear debris trapped between the protruding N-fibres was instrumental in lowering the wear rate. However, this mechanism is cyclic. Large bending stresses at the protruding tips tend to fracture the fibres at points below the surface of the composite. These fractured pieces are then pulled-out of the matrix.

The phenomenon of wear debris entrapment is a vital mechanism in mitigating wear. Transfer films seemed to offer protection to fibre orientations that needed it most. In the case of woven surfaces with AP-oriented fibres, wear debris consisting of cohered particles of the worn matrix was trapped between the fibres. This deposit grew until it covered the fibres,

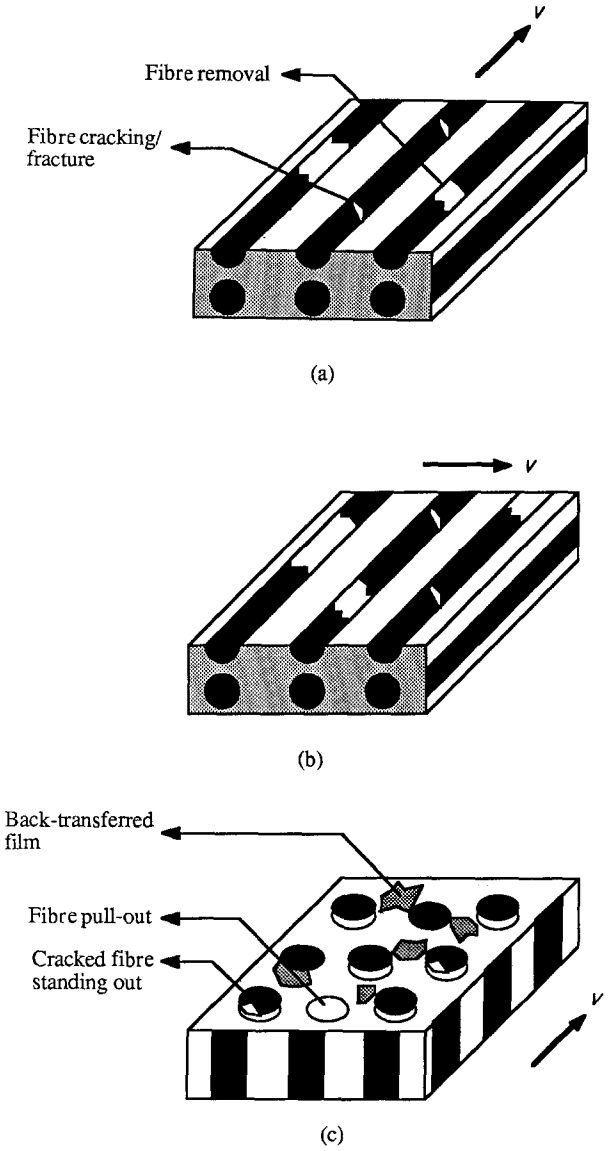

Figure 24 Model for wear of the unidirectional composite: (a) P-orientation, (b) AP-orientation, and (c) N-orientation.

which action shielded them from the microcutting mechanism by the steel asperities. This resulted in an equivalence of wear rates of the P/AP and AP/P woven surfaces. This statement is readily appreciated in Figs 25 and 26. These schematic drawings highlight the relevance of the microstructure of the woven composite to its enhanced friction and wear resistance. The following discussions pertain to two classes of woven composites: (a) one with only P- and AP-oriented fibres (P/AP and AP/P surfaces) – Figs 25a and b, and (b) one with N-oriented fibres as one of the constituent fibres (N/P and N/AP surfaces) – Figs 26a and b. The former type had demonstrated greater wear resistance than the latter.

4.2.1. P/AP or AP/P woven surfaces

Firstly, the very nature of the weave causes the fibre bundles to hold themselves and each other on the surface. Secondly, the cross-over points act as a concentration site for wear debris thereby, causing only these regions to be in strong contact with the counterpart. The other regions are hence, protected from severe wear. At regions further away from the point of crimping, and over a small area in the middle of the cross-over, the fibres are perfectly parallel and transverse, respectively. In fact, the area occupied by these two orientations is so large that the woven surface could be approximated by a mosaic of these two regions. Such an approximation, which leads to the application of a rule-of-mixtures approach, ignores the effect of bending of fibres on all four sides of the point of crimping. Quite naturally, this is the reason for its failure of application to sliding wear.

As shown in Fig. 25a, in the case of the three specific P-oriented fibre bundles, and in Figs 17 and 18 which showed a single fibre bundle far away and close, respectively, to the region of cross-over, it can be conclusively said that wear in these composites occurs

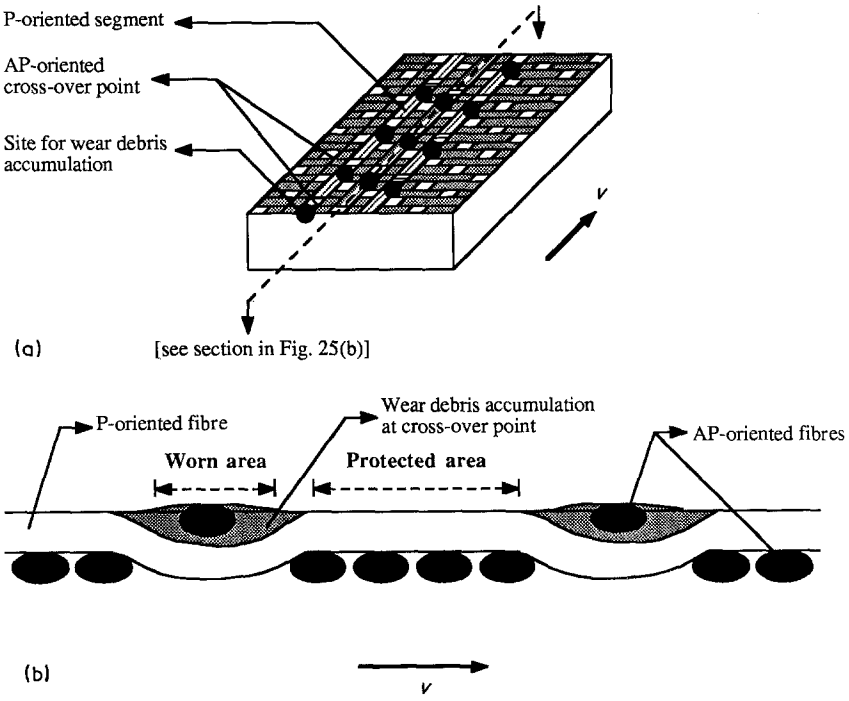

Figure 25 Model for wear of the P/AP woven composite: (a) sliding surface, (b) transverse view of a cross-over point.

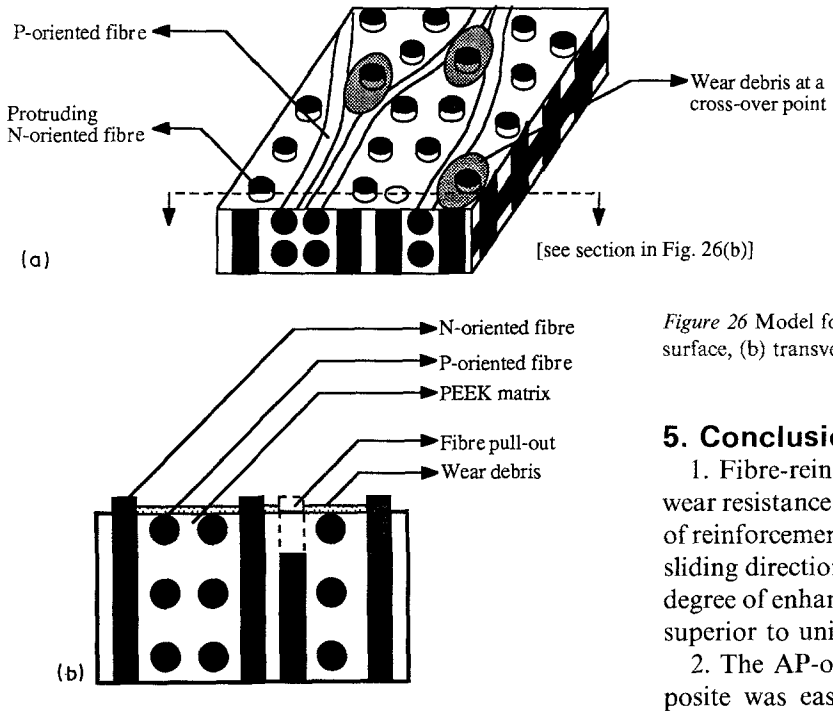

Figure 26 Model for wear of the N/P woven composite: (a) sliding surface, (b) transverse view of the sliding surface.

primarily at these regions. Moreover, the presence of AP-oriented fibres at these regions acts in a beneficial way to trap the back-transferred worn polymer. An elevation in the surface due to the crimping of the fibres is therefore essential in reducing wear, as is evident from Fig. 25b. As wear progresses, the initial cross-over points get worn. Simultaneously, new cross-over points are generated; these, in turn, attract wear debris, and hence, the process of wear protection continues.

4.2.2. N/P or N/AP woven surfaces

Wear-resistance enhancement by wear debris entrapment also occurred in this case, as shown in Fig. 26a. There are yet two fundamental differences in the method of wear resistance. Firstly, there is no effect of a "holding together" by fibre bundles on the sliding surface, and secondly, the wear shielding process is cyclic, and generates more wear. Nevertheless, the wear debris, besides imparting lubricating effects, also serves two other beneficial causes. On the one hand, it cushions the composite surface and reduces the load on the N-fibres, and hence, the bending stresses on them. This, in turn, reduces the tendency for fracture. Secondly, by occupying the regions between the N-fibres, it actually protects these regions from direct wear and frictional effects.

It may be noted, however, that in both the orientations, there were instances when pieces of steel were picked up from the counterface and embedded in the specimen surface. The embedment usually occurred near the edges of the specimens, and caused severe damage to not only the composite (by way of a re-deposited steel particle on the counterface producing a groove), but also to the steel counterface (by way of generating a local steel-on-steel micropair and scoring the surface). In addition, extensive damage was also effected in the regions around the embedded particles.

5. Conclusions

1. Fibre-reinforcements improved significantly the wear resistance of the unreinforced polymer. The form of reinforcement and its orientation with respect to the sliding direction played a vital role in determining the degree of enhancement; woven fibres proving to be far superior to unidirectional fibres.

2. The AP-orientation for the unidirectional composite was easily the least wear resistant case and yielded wear rates that were much higher than for the other two orientations. Although the P and N-orientations were close in wear rates, damage was less in the former case which proved to be the most wear resistant orientation. Wear rates increased linearly with *pv* values, and also with temperature, the gradation in properties with respect to sliding orientations being maintained throughout the range of the testing parameters. The coefficients of friction, on the other hand, did not vary significantly with orientation, but increased slightly with increases in *pv* values.

3. Wear rates for the woven composite were an order-of-magnitude lower than for the unidirectional composite. While they increased markedly with both *pv* and temperature, variance among the different orientations was not significant. However, from the damage point of view, the P-orientation which comprised of 80% in-plane fibres parallel and 20% in-plane fibres transverse to the direction of sliding constituted the most wear resistant case, while the (N, AP) orientation, in spite of its almost comparable wear rate, was prone to considerable fibre damage.

4. Generally, the wear behaviour of composite specimens possessing N-oriented fibres (in any proportion) tended to be an almost unfavourable case. These fibre bundles were able to score out pieces of the steel counterface, which got embedded into the matrix surface. By producing a local steel-on-steel sliding micro-pair, severe scoring of the counterface was effected.

5. The coefficients of friction were largely independent of fibre orientation, and increased marginally with *pv* and temperature up to 150° C. At 240° C, extremely high coefficients were observed, largely due to the fact that the material was near its "limiting *pv*" value for that combination of testing parameters.

Acknowledgements

P. B. Mody and Dr T. W. Chou thank the US Army Research Office for supporting this project. Dr K. Friedrich thanks the German Science Foundation

(DFG) for supporting his activities in this research by DFG 675-1-2.

References

1. P. B. MODY, MS thesis, University of Delaware (1987).
2. P. B. MODY, T. W. CHOU and K. FRIEDRICH, in ASTM STP 1003 "Test Methods and Design Allowables for Fiber Composites" edited by C. C. Chamis (American Society for Testing and Materials, Philadelphia, Pennsylvania, 1987).
3. K. FRIEDRICH and M. CYFFKA, *Wear* **103** (1985) 333.
4. M. CIRINO, K. FRIEDRICH and R. B. PIPES, *J. Mater. Sci.* **22** (1987) 2481.
5. K. TANAKA, *J. Lubric. Technol.* **99** (1977) 408.
6. J. C. ANDERSON, *Tribology Int.* **10** (1982) 255.
7. M. P. WOLVERTON, J. E. THEBERGE and K. L. McCADDEN, in Proceedings of 38th Annual RPI Conference, February 1983 (SPI, Society for Plastics Industry, Washington, DC, 1983).
8. H. CZICHOS, *Wear* **88** (1983) 27.
9. J. K. LANCASTER, *J. Phys. D* **1** (1968) 549.
10. K. FRIEDRICH, in "Proceedings of the International Conference on Wear of Materials", Vancouver, Canada, April 1985, edited by K. C. Ludema (American Society of Mechanical Engineers, New York, 1985) p. 751.
11. H. VOSS and K. FRIEDRICH, *Wear* **116** (1987) 1.
12. H. M. HAWTHORNE, in "Proceedings of the International Conference on Wear of Materials", Vancouver, Canada, April 1985, edited by K. C. Ludema (American Society of Mechanical Engineers, New York, 1985) p. 576.
13. T. H. GROVE and K. G. BUDINSKI, in "Wear Tests for Plastics: Selection and Use", ASTM STP 701, edited by R. G. Bayer (American Society for Testing and Materials, Philadelphia, Pennsylvania, 1979) p. 59.
14. M. N. GARDOS, A. A. CASTILLO, J. N. HERRICK and R. A. SODERLUND, in "Proceedings of the 3rd International Conference on Solid Lubrication", Denver, Colorado, August 1984 (ASLE, Park Ridge, Illinois, 1984) p. 248.
15. B. BRISCOE, *Tribology Int.* **9** (1981) 231.
16. K. FRIEDRICH, in "Friction and Wear of Polymer Composites", edited by K. Friedrich (Elsevier Science, Amsterdam, 1985) p. 233.
17. H. VOSS, K. FRIEDRICH and R. B. PIPES, in "Proceedings of the International Conference on Wear of Materials", Houston, Texas, April 1987, edited by K. C. Ludema (American Society of Mechanical Engineers, New York, 1987).
18. Z. ELIEZER, V. D. KHANNA and M. F. AMATEAU, *Wear* **51** (1978) 169–179.

Received 5 October 1987
and accepted 26 January 1988